Synthesis, photophysical, electrochemical, and electrochemiluminescent properties of 5,15-bis(9-anthracenyl)porphyrin derivatives†

Chloè Sooambar,[a] Vincent Troiani,[b] Carlo Bruno,[c] Massimo Marcaccio,[c] Francesco Paolucci,*[c] Andrea Listorti,[d] Abdelhalim Belbakra,[d] Nicola Armaroli,*[d] Alessandra Magistrato,*[e] Rita De Zorzi,[f] Silvano Geremia[f] and Davide Bonifazi*[a,b]

Received 12th November 2008, Accepted 10th March 2009
First published as an Advance Article on the web 16th April 2009
DOI: 10.1039/b820210a

Novel 5,15-bis(9-anthracenyl)porphyrin derivatives (**1a**, **1b**) were synthesized by stepwise Suzuki-type coupling reactions using anthracenyl-boronates bearing various electronically active moieties. Absorption spectra of these porphyrin conjugates reveal some degree of delocalisation with the directly linked chromophores, particularly in the case of anthracenyl-porphyrin bearing dimethylanilino moieties at the two extremities. Fluorescence and 77 K phosphorescence properties indicate that the excitation energy is invariably funnelled to the lowest singlet and triplet states of the porphyrin chromophore. The latter levels have been probed also by transient absorption spectroscopy, showing the typical triplet features detected in *meso*-substituted porphyrins. Extensive electrochemical studies have been performed to unravel the electronic properties of the newly synthesized porphyrins. Low-temperature cyclic voltammetry investigations showed that the anthracenyl-porphyrins are capable of undergoing as many as four electron transfer processes. In particular, by means of UV-Vis-NIR spectroelectrochemical measurements, a NIR-centred intramolecular photoinduced intervalence charge transfer (IV-CT) from a neutral *N*,*N*-dimethylanilino moiety to the *N*,*N*-dimethylanilino radical cation has been observed for the doubly-oxidised porphyrin **1b**$^{2+}$. The molecules also showed unexpected electrogenerated chemiluminescence properties, which revealed to be largely controlled by the electronic characteristics of the peripheral anthracenyl substituents. The structural and the electronic properties of these complexes have been also characterised by DFT calculations, as well as by X-ray crystallographic analyses.

Introduction

Understanding the electronic communication among the π-conjugated constituents of multicomponent architectures is essential toward the development of new organic materials for several applications including light-harvesting antennae and photosynthetic reaction centres, light-emitting diodes, photovoltaic cells, field-effect transistors and non-linear optics.[1,2] In particular, molecules in which both distance and orientation between electronically-active donor and acceptor functions are accurately known provide a useful vehicle for understanding the mechanism of electron and/or energy transfer.[1,3] In this respect, a great deal of academic and industrial research is focused on the development of new tuneable electrochemiluminescent organic materials with the aim of fabricating organic light emitting devices (LEDs).[4–6] The basic requirements for an organic electroluminescent material are the capability to undergo charge transfer to an electrode, to transport electron/holes in the solid phase and to emit visible light following electrical stimulation.[5,7] Tuning the energy gap between the highest occupied molecular orbital (HOMO) and the lowest unoccupied molecular orbital (LUMO) plays a crucial role in optimizing the performances and properties of the materials because it allows suitable matching of the device interfaces.[5]

With their unique photophysical properties in the ground and excited states, porphyrins are very successful functional molecular modules.[8,9] Their electronic features are largely exploited to design optical materials and devices.[10,4,11] Notably, their narrow HOMO-LUMO gaps (if compared to the other monomeric aromatic scaffolds) make them very attractive modules for the construction of large π-conjugated molecules in which the electronic properties can be extensively tuned by varying the macrocycle porphyrin peripheral substituents or by selecting the central metal ion.[12,13,14] Porphyrins have been largely used in multicomponent

[a]*Università degli Studi di Trieste, Dipartimento di Scienze Farmaceutiche and INSTM UdR Trieste, Trieste, Italy. Fax: 0039 040 52527*
[b]*University of Namur (FUNDP), Department of Chemistry, B-5000 Namur, Belgium. E-mail: davide.bonifazi@fundp.ac.be; Fax: 0032 (0)81 725433*
[c]*Molecular Photoscience Group, Istituto per la Sintesi Organica e la Fotoreattività del CNR, via P. Gobetti 101, Bologna, Italy. E-mail: armaroli@isof.cnr.it; Fax: 0039 051 6399844*
[d]*CNR-INFM Democritos Center and International School for Advanced Studies (SISSA/ISAS), Trieste, Italy. E-mail: alema@sissa.it; Fax: 040-3787-528*
[e]*Università degli Studi di Bologna, Dipartimento di Chimica "G. Ciamician", Bologna, Italy. E-mail: francesco.paolucci@unibo.it; Fax: + 39-051-2099456*
[f]*Università degli Studi di Trieste, Dipartimento di Scienze Chimiche, Center of Excellence in Biocrystallography, Trieste, Italy. Fax: +39 040 558 3903*

† Electronic supplementary information (ESI) available: Experimental, X-ray data, absorption and emission spectra, structural parameters, Kohn–Sham orbital diagrams and ^{1}H NMR spectra. CCDC reference numbers 631312 and 716280. For ESI and crystallographic data in CIF or other electronic format see DOI: 10.1039/b820210a

assemblies in which the photo- and/or electroactive units are fixed in a certain spatial orientation.[15] They have mainly been connected following three approaches: coordination through the metal centre, weak intermolecular interactions through the organic framework (*e.g.* hydrogen bonds) or covalent bonding through rigid spacers.[8,13,16] While the non-covalent approach often leads to weak electronic coupling extended to one-,[17] two-,[18] and three-dimensional[19] supramolecular structures, the covalent strategy allows fine-tuning of the electronic interaction. Typically this is accomplished by choosing covalent spacers that can vary in size, shape, and electronic structure. Therefore, the choice of the appropriate substituent and/or linkage is the key step in the design of multicomponent porphyrin-based ensembles.

The present work focuses on the synthesis, optical, electrochemical, and electrochemiluminescent properties of conjugated 5,15-bis(9-anthracenyl)porphyrin Zn complexes (**1a–b**, Scheme 1) that featured orthogonal anthracenyl moieties displaying various degrees of electronic density as also shown by comprehensive computational modelling performed at the DFT/BLYP level of theory. Fluorescence, including quantum yields and lifetimes, and 77 K phosphorescence properties along with transient absorption spectroscopy indicate that the excitation energy is invariably funnelled from the anthracenyl moieties to the lowest singlet and triplet states of the porphyrin chromophore. Comprehensive electrochemical investigations revealed that all porphyrin-anthracenyl derivatives are capable of undergoing reversible multiple electron-transfer processes, the energy of which is controlled by the peripheral anthracenyl substituents. Moreover, the molecules showed unexpected electrogenerated chemiluminescence properties in solution, which is also controlled by the electronic characteristic of the peripheral anthracenyl substituents.

Results and discussion

Synthesis

Attempts to covalently link tetrapyrrolic macrocycles to highly fluorescent units such as anthracenes, have been mainly limited to position 1[20] because of the difficulties in preparing on a large scale *meso*-substituted 9-anthracenyl porphyrins *via* a classical condensation reaction starting from 9-anthraldehyde and pyrrole due to steric limitations occurring during the porphyrinogen formation step.[21] Therien and co-workers firstly reported a porphyrin functionalized at the β-position with a 9-anthracenyl moiety,[22] while very recently Anderson and co-workers reported the first mono-functionalisation of porphyrin derivatives at the *meso*-position.[23] The target compounds **1a–b** were obtained by Suzuki-type cross-coupling between diiodo-porphyrin **2** (which has been prepared by iodination of porphyrin **3** in the presence of I_2 and $AgPF_6$)[24,25] and boronates **4a–b**, respectively, in the presence of $[Pd(PPh_3)_4]$ and Cs_2CO_3 in PhMe/DMF at reflux temperature (Scheme 1).[25] Addition of DMF as a co-solvent was crucial to obtain the final compounds. Precursors **4a–b** were prepared by using 4,4,4′,4′,5,5,5′,5′-octamethyl-2,2′-bi(1,3,2-dioxaborolane) and **5a–b**, respectively, in the presence of $[Pd(PPh_3)_4]$ and AcOK in PhMe. Reference porphyrin derivative **7** was also synthesised following the same synthetic methodology as that used for **1a**. All compounds were isolated by flash column chromatography on silica gel and were fully characterised by ^{1}H-and ^{13}C-NMR, X-ray, FT-IR and UV-visible spectroscopy.

Single crystals of porphyrins **1a–b** were grown by slow diffusion of H_2O into MeOH \ CH_2Cl_2 and MeOH \ Pyr \ $CHCl_3$ solutions for **1a** and **1b**, respectively, and used for X-ray crystal structure analyses (Fig. 1a–b). The unit cell for the crystal of molecule **1a** is triclinic with $P\bar{1}$ symmetry whereas **1b** is monoclinic with

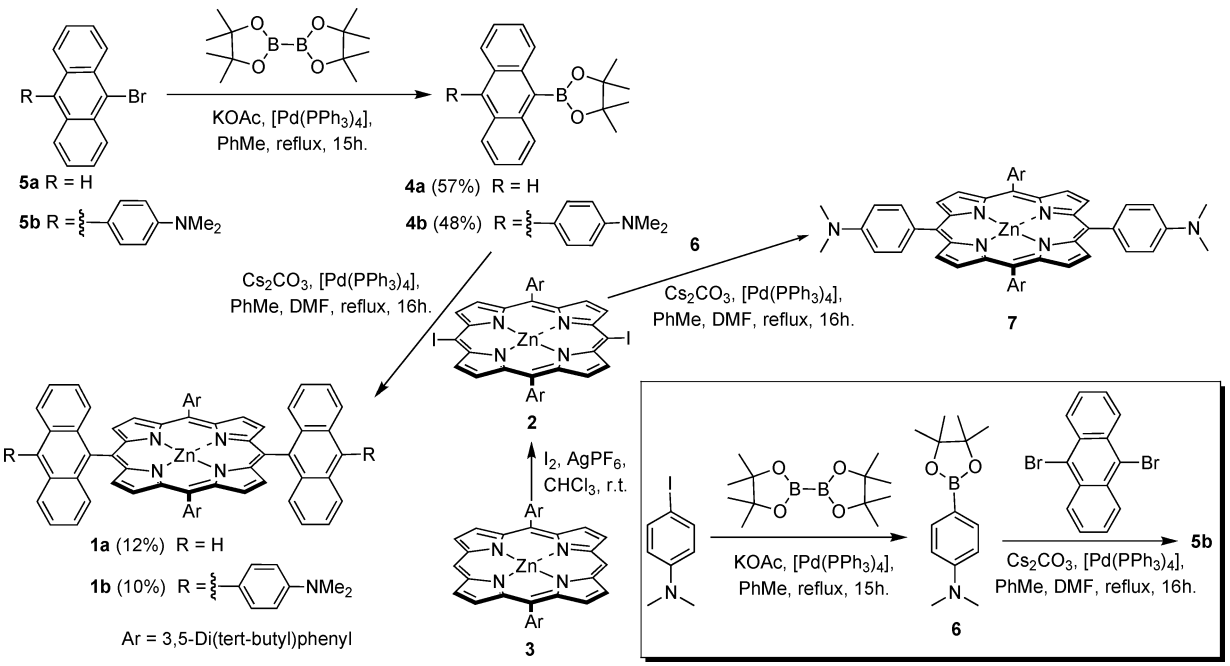

Scheme 1 Synthesis of the *N*,*N*′-dimethylaniline-bearing 5,15-bis(9-anthracenyl)porphyrins. Ar = 3,5-Di(*tert*-butyl)phenyl.

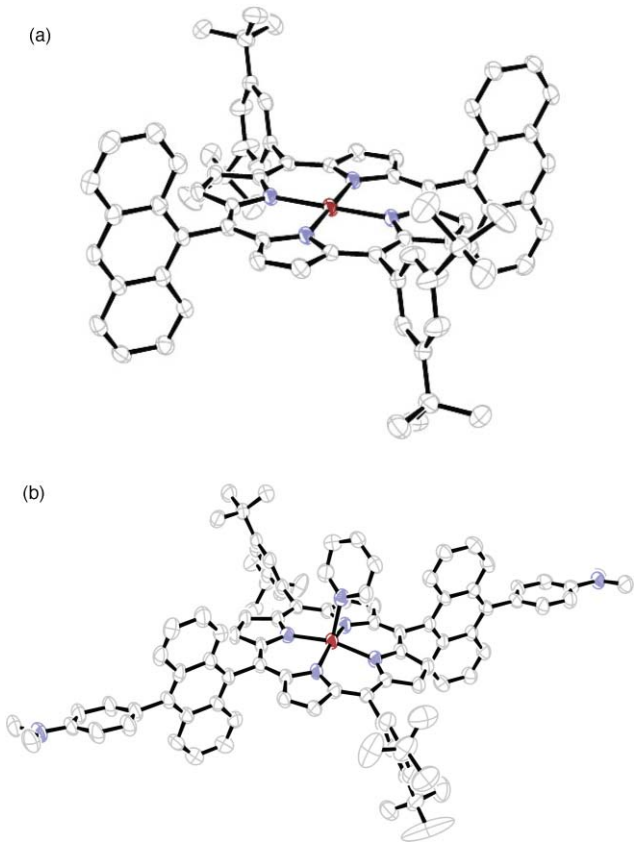

Fig. 1 Molecular structure of **1a** (Fig. 1a) and **1b** (Fig. 1b) in the crystal. Atomic displacement parameters obtained at 233 K are drawn at the 50% probability level. Atom colours: blue N, grey C, red Zn.

C2/c symmetry. The refinement was performed by introducing 2.5 molecules of CH_2Cl_2 in the asymmetric unit for **1a** and three $CHCl_3$ molecules, among which two were partially disordered, and half a molecule of CH_2Cl_2 for **1b**. The electron density maps and the refinement of the structures revealed in the asymmetric unit the presence of a half porphyrin molecule in **1a** (*i.e.*, Zn atom of the porphyrin lies on an inversion centre) and a whole macrocycle in **1b**, with the Zn(II) ion coordinated in the centre of the tetrapyrrole ring with an average Zn–N distance of 2.04 and 2.06 Å for **1a** and **1b**, respectively. For porphyrin **1b**, the metal ion makes an extra coordinative Zn–N contact of 2.15 Å with a molecule of pyridine orthogonally nested atop the porphyrin ring. The fifth coordination caused a displacement of the Zn(II) ion out of the porphyrin plane of 0.33 Å towards the pyridine ligand. The X-ray crystal structures reveal the nearly orthogonal arrangement of the 9,10-anthracenyl moieties with respect to the porphyrin ring and, for molecule **1b**, also orthogonal to the terminal *N*,*N*-dimethylanilino residues. The plane of the two aryl groups is twisted of about 64° and 90° with respect to the tetrapyrrolic ring, for **1a** and **1b**, respectively.

Photophysical studies

The electronic absorption spectra of porphyrin derivatives **1a–b** and **7** in toluene (PhMe) solutions are depicted in Fig. 2a, in comparison with the reference porphyrin system **3**.[25] Both the intense Soret band around 420 nm and the whole Q-band envelope are red-shifted by 25–30 nm suggesting electronic ground state delocalisation with the directly linked chromophores, namely anthracene, aniline, and *N*,*N*-dimethylanilino-anthracene. The perturbative effect is particularly strong with the aniline residue (**7**) where broadening of the Soret band and strong variations in the relative intensity of the *Q* transitions are peculiarly observed. Comparison of the spectra of the conjugates with the summation of the spectra of the component units (Fig. S1†) also emphasizes the substantial conjugation of the two moieties; in particular, the anthracenyl-centred absorption around 350 nm is strongly reduced and largely masked by the porphyrin-centred absorption in molecules **1a–b**.

Table 1 Photophysical data in PhMe

	298 K			77 K		
		Fluor.		Fluor.	Phospho[a]	
	λ_{max} [nm]	τ [ns]	Φ	λ_{max} [nm]	λ_{max} [nm]	τ [ms]
4a	428	6.8	0.48	417	[c]	[c]
6	336	3.2	0.08	336	419	1200
4b	465	0.5,5.7	0.08	451	[c]	[c]
3	632[b]	2.5	0.02	631	742	51
1a	648[b]	2.55	0.02	648	770	35.6
7	616[b]	1.8	0.03	628	790	27.4
1b	648[b]	2.4	0.02	598	770	23.8

[a] Emission recorded with a delay of 0.02 ms to cut off the shorter lived fluorescence signal. [b] From the fluorescence spectrum corrected for the detector response. [c] No emission detected.

The relatively intense fluorescence spectra of **1a–b** and **7** in PhMe are depicted in Fig. 2b and are attributable to deactivation from the porphyrin singlet upon comparison with porphyrin reference **3**; the spectra of the 5,15-bis(9-anthracenyl)porphyrins **1a–b** are virtually superimposable. Detailed photophysical data, including fluorescence quantum yields, singlet lifetimes at 298 K and phosphorescence data at 77 K are collected in Table 1. Spectral onsets of singlet and triplet emission features are slightly red-shifted in the three conjugates relative to porphyrin reference **3**, in line with the absorption trends. The emission spectral shapes are very similar to the reference compound, except for molecule **7**, also in analogy with absorption spectra. The latter compound exhibits the shortest singlet lifetime and the largest fluorescence quantum yield (Table 1). Porphyrins **1a–b** and **7** show a long-lived (ms timescale) emission band above 700 nm at 77 K, attributed to deactivation of the lowest lying porphyrin-centred triplet,[26] in analogy with porphyrin precursor **3**.

In general, the emission properties of porphyrins **1a–b** and **7** are similar to each other and comparable to those of **3** (Table 1). Notably, all of the fragments appended to the porphyrin unit are even more powerful fluorophores than the porphyrin reference **3** itself (Table 1, Fig. S2†), but the related singlet levels are quenched in the conjugates. The energy content of the singlet level of each fragment can be estimated from the highest energy fluorescence feature. The porphyrin singlet of molecule **3** is located at approximately 2.1 eV (580 nm), *i.e.* substantially lower lying than those of the molecular substituents **4b**, **5a**, and **6** all placed well above 2.6 eV (Table 1). Hence, singlet energy transfer may take place in the conjugates. At 77 K triplet energy transfer also occurs to the low lying porphyrin triplet (*ca.* 1.6 eV) from the upper lying

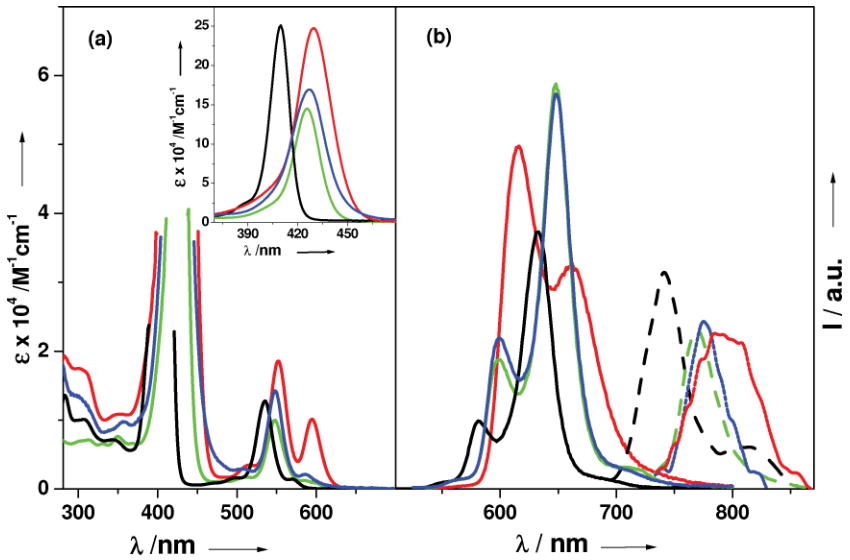

Fig. 2 Absorption (a) and emission (b) spectra of **3** (black), **1a** (green), **1b** (blue), **7** (red) in toluene (PhMe). The intense Soret absorption bands are magnified in the inset. Fluorescence bands are recorded in PhMe and corrected for the detector response (full lines); phosphorescence bands (dashed lines) are taken in 77 K PhMe rigid matrix.

triplets of substituent **6** (>2.9 eV) and the anthracenyl moiety (*ca.* 1.8 eV).[27]

The nanosecond transient absorption spectra of porphyrins **1a–b**, **3**, and **7** in O_2-free toluene solutions are reported in Fig. 3. They are very similar to each other and exhibit the classical profile of porphyrin triplets[28] in the tens of microsecond timescale (see Fig. 3). These findings are in line with those of *meso*-substituted porphyrins[29] and confirm the strong similarities among the various systems, as observed for the singlet excited state properties.

Computational studies

To shed further light upon the origin of the electronic properties of porphyrins **1a–b**, we carried out computational studies employing the CPMD program[30] package at the DFT/BLYP[31,32] level of theory and Gaussian 03 program package[33] with 6-31G basis set and the B3LYP exchange correlation functional.[32,34] Selected structural parameters of molecules **1a** and **1b** are reported in Table S3,† and show that the structure of the central porphyrin

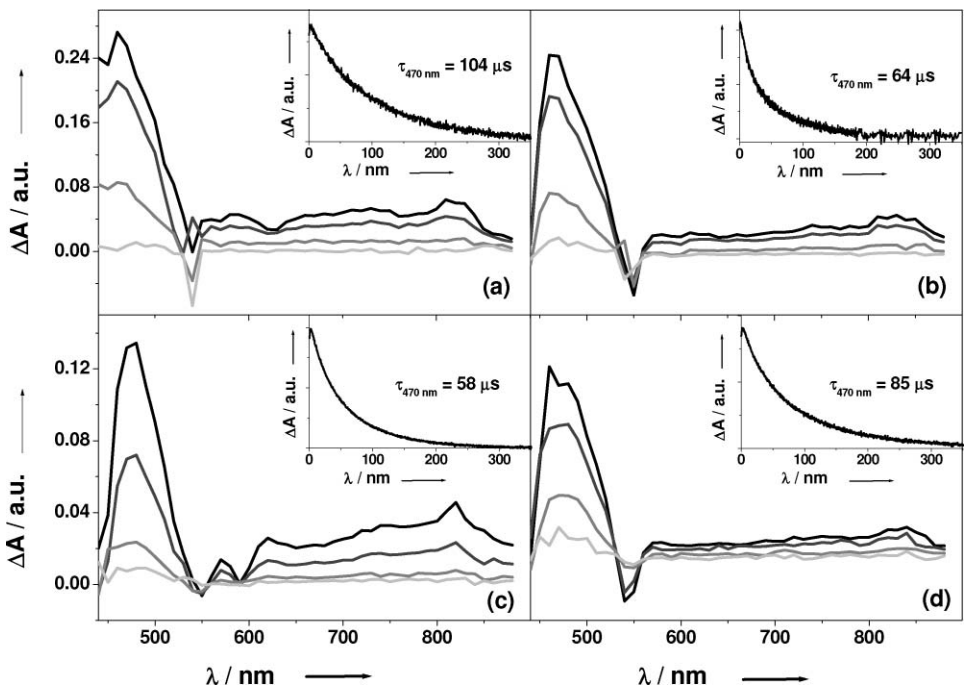

Fig. 3 Transient absorption spectra of **3** (a), **1a** (b), **7** (c), **1b** (d) recorded at 1, 12, 65 and 180 ms after laser excitation in oxygen-free PhMe solution. Insets: transient absorption decays at 470 nm; $\lambda_{exc} = 532$; $E = 1$ mJ/pulse.

complexes is not affected by the presence of the dimethylanilino substituents. In addition, the geometries are rather insensitive to the exchange correlation functional used in the calculations. The only bonds that change substantially are the Zn–N bonds, which are revealed to be slightly overestimated in the BLYP calculations,[35] while the tetrapyrrolic rings are almost identical. Differences are, however, observed in the electronic structures of both porphyrin arrays **1a–b**.[36] In porphyrin **1a**, the Kohn–Sham HOMO and the LUMO orbitals are localised over the tetrapyrrolic rings (Fig. 4 and Fig. S3–4†) as opposite to porphyrin **1b** in which, due to the presence of the peripheral electron donating substituents, the HOMO is localised on the *N*,*N*-dimethylanilino-anthracenyl moiety, while the LUMO is localised on the central rings (Fig. 4 and Fig. S3–4†). Considering also the Hartree–Fock molecular orbitals (Fig. 4 and Fig. S3–4†) calculated on the same optimised geometries (the same orbitals were observed also on Hartree–Fock optimised geometries) we observe that the HOMO and the LUMO of **1a** are unaltered, while in porphyrin **1b** the HOMO involves the central porphyrin rings. However, small differences are observed in the energies of the highest occupied states, which make their relative energies highly dependent on the level of theory. In fact, a relative shift in energies of the orbitals close to the HOMO and LUMO is observed in the Hartree–Fock and Kohn–Sham orbitals for both molecules. Thus, we should remark that this provides only a qualitative picture of the electronic structure of the molecules. We have also considered complexes **1a** and **1b** in their single and double oxidation states (Table S3†). B3LYP optimised geometries show a small shortening of the C3–C4 bonds as the oxidation proceeds, which comes along with a progressive change of the torsional angles between the tetrapyrrolic ring and the anthracenyl moieties (Table S3). In molecule **1b** this feature mainly involves the torsional angles between the dimethylanilino and the anthracenyl moieties. As the oxidation proceeds, the torsional angles progressively depart from 90°. The electronic structure analysis of the oxidised complexes reveals that the HOMO orbital localised on the tetrapyrrolic rings of **1a** moves on the anthracenyl rings upon single and double oxidation, while the LUMO orbitals of **1a** and **1a**$^{+}$ are similar and localised on the tetrapyrrolic ring and that of **1a**$^{2+}$ is completely delocalised on the different moieites. In contrast, the HOMO orbital is always localised on both *N*,*N*-dimethylanilino-anthracenyl substituents upon single and double oxidations, while the LUMO localised on the tetrapyrrolic rings in the neutral and the singly-oxidised state becomes delocalised over the *N*,*N*-dimethylanilino-anthracenyl substituents at the second oxidation. The electronic structure of the oxidised species is consistent for both DFT and Hartree–Fock level of theory.

Electrochemistry

To assess the electronic properties of **1a–b**, their electrochemical behaviour was investigated in tetrahydrofuran (THF), with

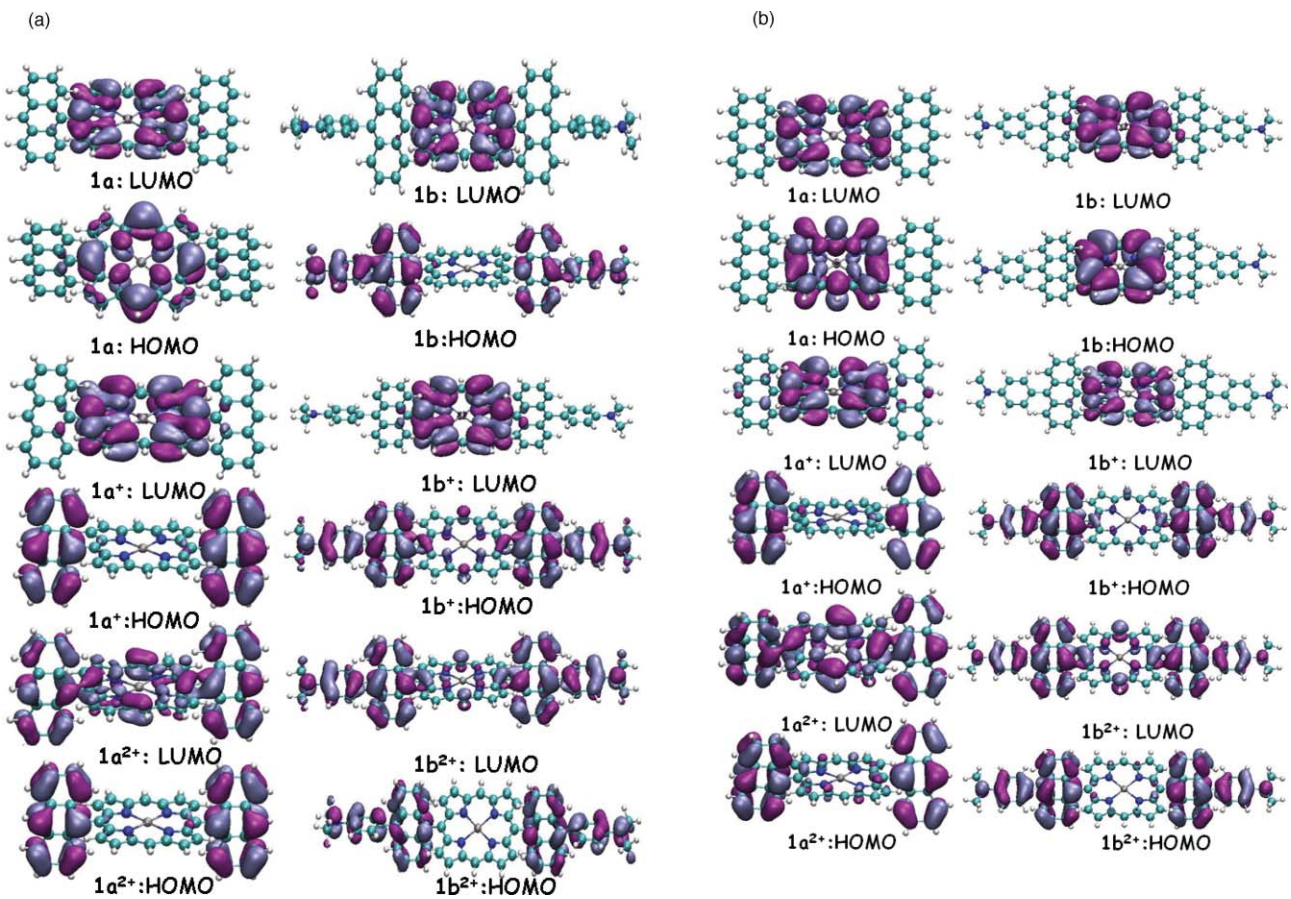

Fig. 4 Kohn–Sham (a) and Hartree–Fock (b) HOMO and LUMO orbitals of **1a**, **1a**$^{+}$, **1a**$^{2+}$, **1b**, **1b**$^{+}$ and **1b**$^{2+}$ (the 3,5-di(*tert*-butyl)phenyl groups have been replaced by H atoms).

tetrabutylammonium hexafluorophosphate (TBAH) as supporting electrolyte. All potentials are referred to SCE. Five reversible redox couples (Fig. 5a) were observed for molecule **1a**: three reductions (at –1.39, –1.80, and –2.19 V) and two oxidations (at 0.96 and 1.31 V). While the two oxidations and the first two reductions were found to correspond to 1-e$^-$ transfer processes, the third reduction corresponds to a 2-e$^-$ process. On the basis of the reported redox behaviour of metallated porphyrins investigated under similar conditions[37,38] and by comparison with the porphyrin model **3** (Fig. 5b), all 1-e$^-$ peaks observed in Fig. 5a are attributed to electron transfer processes involving the tetrapyrrolic ring, while the 2-e$^-$ couple is associated to the reversible reduction of the two 9-anthracenyl residues. The introduction of the two peripheral *N*,*N*-dimethylanilino moieties in position 10 of each anthracenyl moiety (**1b**) led to a dramatic change of the voltammetric properties (Fig. 5c). While the cathodic processes, *i.e.* the reductive processes, display a similar pattern (two 1-e$^-$ and one 2-e$^-$ reduction peaks at –1.39, –1.80 and –2.19 V, respectively) to that observed for **1a**, the anodic processes are radically different. The first oxidation peak observed at positive potentials (0.95 V) corresponds in fact to the superimposition of two 1-e$^-$ transfer processes occurring at very close potentials, as typically observed in the presence of two identical and weakly-interacting redox centres. In view of their chemical equivalency, such a peak might then involve the peripheral *N*,*N*-dimethylanilino-anthracenyl moieties rather than the central porphyrin core. On the other hand, the peak is located at nearly the same potential as in molecule **1a**, where its attribution to a porphyrin-centred process is unequivocal. The hypothesis can then be made that the two oxidation processes comprised in such a peak involve each one of the two above moieties, *i.e.* either the central porphyrin ring or one of the *N*,*N*-dimethylanilino residues. In line with this hypothesis, low-temperature CV measurements (Fig. 5d) show a partial resolution of the 2-e$^-$ oxidative peak thus suggesting different temperature coefficients (*i.e.*, different electron transfer entropies) for the two redox processes (the estimated $E_{1/2}$ of which are 0.94 and 1.04 V), as expected if electrochemically non-equivalent redox moieties are involved. All data have also been interpreted by computational studies (*vide supra*). The picture provided by the electrochemical data is consistent with the HOMO orbitals obtained at the Hartree–Fock level for **1b** and **1b**$^+$ (Fig. 4a and Fig. S4†) displaying that the two first oxidative processes (*i.e.*, at 0.94 and 1.04 V) occur at the tetrapyrrolic and anthracenyl moieties, respectively. The same qualitative picture is also observed for **1a** (Fig. 4b and Fig. S3†), although this is not fully consistent with the experimental results. However, we should take into account that the small energy differences between the highest occupied states make this calculation qualitative and cannot be considered, in this case, of absolute interpretation. Additionally, at low-temperature, two more 1-e$^-$ oxidation peaks (at 1.23 and 1.46 V, respectively) were observed at more positive potentials, which could be attributed to either the second oxidation of the porphyrin core or to the oxidation of the second *N*,*N*-dimethylanilino moiety. Interestingly, such peaks display a significant larger half-peak width than the preceding peaks thus suggesting an increased activation barrier for these charge transfer processes. The separation between the second and third process (190 mV) is significantly smaller than that between the successive oxidations of the porphyrin core in molecules **1a** (350 mV) and **3** (370 mV): the process at 1.23 V would then correspond to the oxidation of the second *N*,*N*-dimethylanilino moiety while that at 1.46 V to the second oxidation of porphyrin.

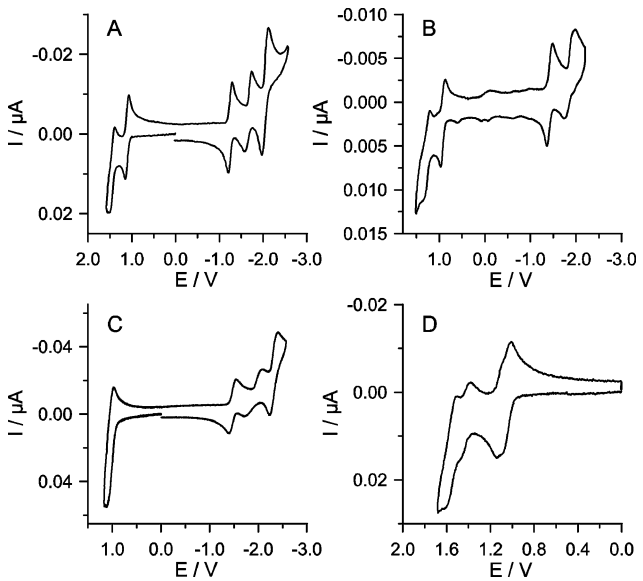

Fig. 5 CV curves of (a) **1a** (0.5 mM), scan rate: 0.4 V s^{-1}, T = –50 °C; (b) **7** (0.5 mM), scan rate: 1 V s^{-1}, T = 25 °C; (c) **1b** (0.5 mM), scan rate: 1 V s^{-1}, T = 25 °C; (d) **1b** (0.5 mM), scan rate: 0.4 V s^{-1}, T = –50 °C. All CVs were performed under ultra-dry conditions.

UV-Vis-NIR spectroelectrochemistry

With the aim of confirming the attribution of the redox processes given above, a UV-vis-NIR spectroelectrochemical investigation of the two bisanthracenyl-porphyrins **1a–b** was carried out at room and low temperature (–35 °C) in THF, under the same strictly aprotic conditions used for the CV studies. Fig. 6a compares the electronic absorption spectra of molecules **1a–b**. The two species show very similar spectra where both porphyrin-centred and anthracenyl-centred transitions are observed. In particular, the B (Soret) band is centred at 431 and 432 nm for **1a** and **1b**, respectively (the Q bands at 557 and 595 nm and at 558 and 596 nm for **1a** and **1b**, respectively). The two anthracenyl moieties are instead responsible for the transition at 255 nm, while the anthracenyl-centred typical, low-intensity, absorption bands in the 300–400 nm range are partly covered by the intense porphyrin B band.[39,40] Fig. 6b and 6c show the absorption spectra of **1a–b** respectively at various applied potentials. At potentials corresponding to the first and second reductions of the complexes, both spectra undergo the typical changes associated to the generation of porphyrin-centred π radical anions and dianions: during the first reduction, small changes are observed in the Soret band and the two Q bands of both species, *i.e.* the bands' intensities decrease and shift to higher wavelengths.[41,42] The second reduction of both complexes brings about more dramatic changes in the spectra, *i.e.* a pronounced intensity decrease of the Soret and Q bands and the appearance of new low-intensity absorption bands at 701–703 nm and 891–893 nm,[38,41,43] also associated to the formation of porphyrin-based dianions. No significant change was observed with the third 2-e$^-$ reduction that, according to the above analysis of CV behaviour, is centred at the anthracenyl fragments: the weak absorption bands of the reduced anthracenyl moieties[39,44]

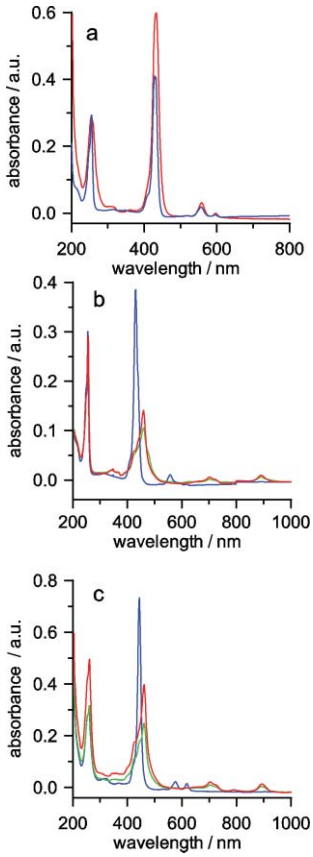

Fig. 6 (a) Thin-layer electronic absorption spectra of porphyrins **1a** (red trace) and **1b** (blue trace) in 0.5 mM in 0.08 M TBAH/THF solutions. (b) Spectral evolution upon exhaustive reduction of **1a** at various potentials: –1.6 V (blue line); –1.8 V (red line); –2.0 V (green line). (c) Spectral evolution upon exhaustive reduction of **1b** at various potentials: –1.6 V (blue line); –1.8 V (red line); –2.0 V (green line). T = 238 K. Potentials are referenced to SCE.

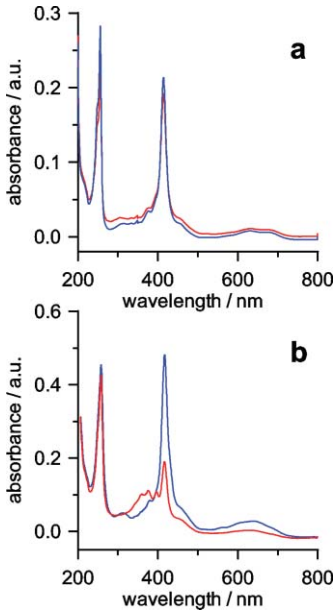

Fig. 7 Thin-layer electronic absorption spectral evolution upon exhaustive oxidation (a) of **1a** at 1.3 V (blue line) or 1.8 V (red line) and (b) of **1b** at 1.1 V (blue line); 1.9 V (red line). T = 238 K. Potentials are referenced to SCE.

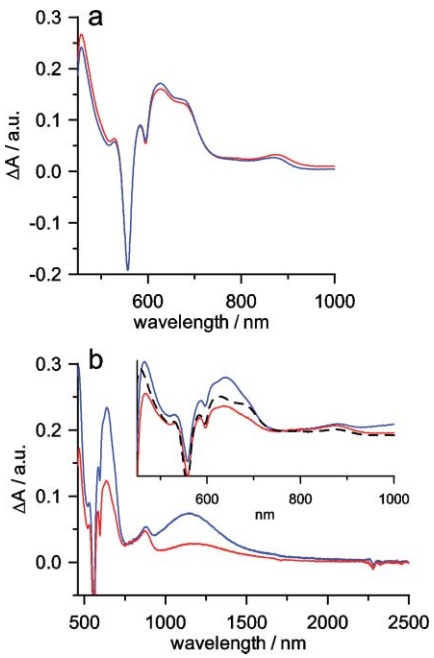

Fig. 8 Difference absorption spectra of (a) **1a** or (b) **1b** solutions, under the conditions of Fig. 2. In the inset, enlarged views (560–1000 nm) of the difference spectra of **1b** at 1.1 V (blue) or 1.8 V (red) and of **1a** at 1.3 V (dashed line) are displayed. T = 238 K. Potentials are referenced to SCE.

are likely masked by the intense bands associated to the porphyrin-based dianion. All spectral changes were totally reversed upon performing the potential-controlled re-oxidation of the porphyrin solutions, confirming the reversibility of all the redox processes in the present conditions, even in the relatively longer time scale of thin-layer bulk electrolysis.

A rather different and, to some extent, unexpected spectro-electrochemical behaviour was found comparing the reversible oxidations of the two porphyrins. Figs. 7a,b compare the UV-vis absorption spectra of porphyrins **1a–b** at potentials corresponding to the first and second oxidations of the two complexes. In the case of **1a** (Fig. 7a), the spectral changes closely match those associated to the generation of the porphyrin-based π cation radical and dication:[45] the Soret bands shift to higher energies with a decreased intensity while the Q bands collapse completely already at the level of the first oxidation. Other changes are observed at longer wavelengths, as illustrated in the difference spectra shown in Fig. 8a. Along with the bleaching associated to collapsing of the Q bands, the broad absorption band with a maximum at 632 nm and a shoulder at 672 nm was unambiguously attributed to the porphyrin-based radical cations by comparison to the reported spectra of similar oxidised porphyrins.[46] The UV-vis absorption spectrum obtained for **1b** at potentials that correspond to its first 2-e$^-$ oxidation (1.1 V) is shown in Fig. 7b (blue line).

It displays spectral changes analogous to those observed for **1a**, thus suggesting that the oxidation involves the porphyrin core with, however, some notable differences both in the 640–680 range (see also Fig. 8b) and in the spectral region between 750 and 2000 nm (Fig. 8b) that deserved a closer inspection. The

increased absorbance in the 640–680 nm range (compare, in the inset of Fig. 8b, the blue and the black dashed trace of $\mathbf{1b}^{2+}$ and $\mathbf{1a}^{+}$, respectively) is attributed to the *N*,*N*-dimethylanilino-centred radical cations that are known to exhibit absorption maxima at around 650 nm.

This is in line with the CV behaviour of molecule **1b**, in which the first 2-e$^-$ oxidative wave would involve, together with the oxidation of the porphyrin core, one of the peripheral *N*,*N*-dimethylanilino moieties. According to such an attribution, an absorption band associated with an intramolecular photoinduced intervalence charge transfer (IV-CT) from a neutral *N*,*N*-dimethylanilino moiety to the *N*,*N*-dimethylanilino radical cation can be expected in the NIR region as revealed by the deconvolution spectra of the absorption profile shown in Fig. 9a. Herein, three distinct bands are observed, at 11524 cm^{-1} (863 nm), 10662 cm^{-1} (938 nm) and 8661 cm^{-1} (1155 nm), respectively. In particular, because of its very large bandwidth (~6000 cm^{-1}), the component at 10662 cm^{-1} is likely to be associated to the above IV-CT transition. As a matter of fact, as molecule **1b** is further oxidised at potentials corresponding to the second set of oxidation peaks, *i.e.* 1.9 V, along with the oxidation of the second *N*,*N*-dimethylanilino moiety, such a band disappears (Fig. 9b).

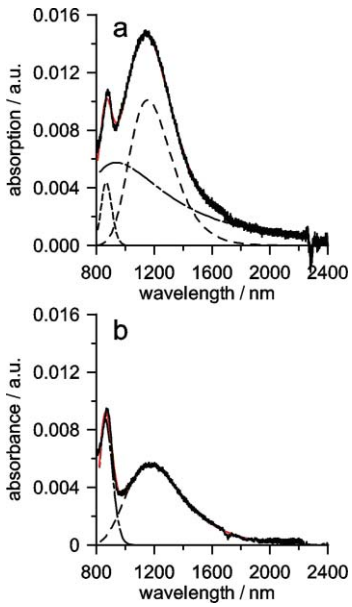

Fig. 9 Absorption spectra of **1b** solutions displaying the gaussian deconvolution (see dashed lines) of the bands in the NIR region: (a) 1.3 V and (b) 1.8 V. The red lines display the reconstructed spectra.

According to the Hush theory,[47] one can deduce the electronic coupling integral, H_{AD}, from the IV-CT band maximum and shape. Assuming an N–N distance between the two *N*,*N*-dimethylanilino moieties of about 2.8 nm, a rather small H_{AD} value of about 120 cm^{-1} is obtained. The band at 11524 cm^{-1}, whose intensity in fact doubles on passing from 2-e$^-$ to 4-e$^-$ oxidised **1b**, is likely to be associated to the *N*,*N*-dimethylanilino radical cation. Finally, the latter process had also small effects on the longest wavelength component of the NIR band, that has shifted by 50 cm^{-1} to higher wavenumbers and the intensity of which has decreased by ~30% (Fig. 9b). Notably, in the final spectrum, the presence of a structured band, with maxima at 359, 376 and 396 nm (Fig. 7b) would suggest the presence of oxidised anthracenyl groups. We can thus infer that, in the higher (>2-e$^-$) oxidised states, **1b** could rearrange to a structure characterised by an expanded π-conjugation where the charge is partly spread throughout the system, and in particular over the anthracenyl moieties. For instance, as testified by the presence of the IV-CT band for the $\mathbf{1b}^{2+}$ species, we can envisage that a partial planarisation of the whole structure would possibly occur for $\mathbf{1b}^{2+}$ through a partial quinoidalisation of the *N*,*N*-dimethylanilino-anthracenyl moieties (see Fig. 10 structures $\mathbf{1b_{qc}}^{2+}$ and $\mathbf{1b_{qt}}^{2+}$), although a fully planar structure would be too strained to form. In order to support this assumption, computational studies were performed on molecule $\mathbf{1b}^{2+}$ in which the two *N*,*N*-dimethylanilino-anthracenyl moieties are rotated by 90 degrees and thus in partial conjugation through a quinoidal form (*i.e.*, which originates the IV-CT band) with the central porphyrin ring. In particular, we have considered either the quinoidal complex $\mathbf{1b}^{2+}$ with both *N*,*N*-dimethylanilino-anthracenyl moieties on the same ($\mathbf{1b_{qc}}^{2+}$) or on opposite sides ($\mathbf{1b_{qt}}^{2+}$) with respect to the plane defined by the tetrapyrrolic ring. Due to the presence of close unfavourable contacts between the anthracenyl and the *N*,*N*-dimethylanilino fragments (shortest close contacts are 1.96 Å for both $\mathbf{1b_{qc}}^{2+}$ and $\mathbf{1b_{qt}}^{2+}$, respectively) both structures turned out to be quite unstable (ΔE = +71 and +86 kcal mol^{-1}, for $\mathbf{1b_{qc}}^{2+}$ and $\mathbf{1b_{qt}}^{2+}$, respectively) with respect to that of $\mathbf{1b}^{2+}$ (*i.e.*, in which the two *N*,*N*-dimethylanilino-anthracenyl substituents are perpendicular). Thus, it is quite unlikely that such compounds could be isolated. Moreover, because of the strain energy associated to the formation of such *quasi*-planar structures, the generating oxidations (*i.e.* the third and/or fourth processes) are likely to be rather slow charge transfer processes, and this is in full agreement with the observed CV behaviours (*vide supra*). Long wavelength absorptions (1100–1200 nm) have also been reported recently for quinoidal porphyrin

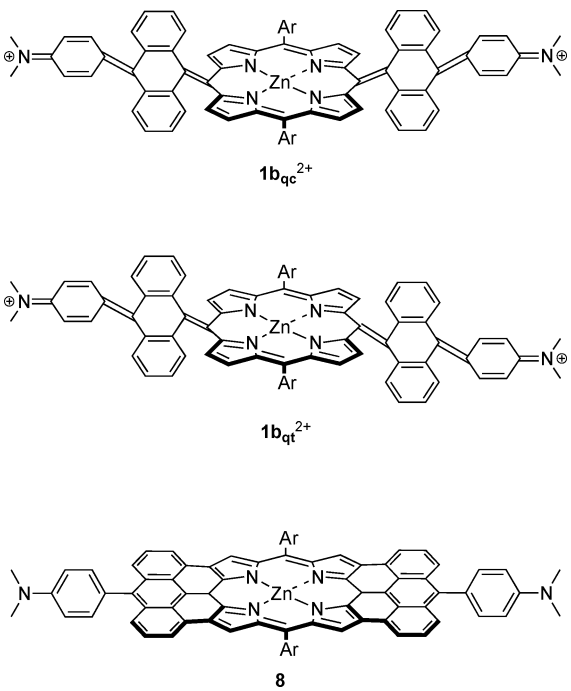

Fig. 10 Planarisation of porphyrin **1b** upon oxidation: formation of quinoidal ($\mathbf{1b_{qc}}^{2+}$ and $\mathbf{1b_{qt}}^{2+}$) and tape-like (**8**) porphyrins.

dimers by Anderson and co-workers,[48] which would support our assumption that the residual NIR absorption observed for the 4-e⁻-oxidised **1b** is caused by a partial planarisation. If we now consider the oxidative fusion between the tetrapyrrolic ring and the two anthracenyl substituents, by removing from 2 up to 8 hydrogen atoms, the tape-like fused anthracenyl-porphyrin derivative **8** (Fig. 10) could be obtained. Considering the reaction with respect to the $\mathbf{1b}^{2+}$, the oxidative fusion of the rings is endothermic at the first step by +1.8 kcal mol^{-1}, and exothermic in the following steps by −7.2, −4.0 and −11.0 kcal mol^{-1} (the properties of the structures corresponding to the progressive fusion of two rings are given in Table S4†). Thus, molecule **8** was revealed to be more stable than $\mathbf{1b}^{2+}$ by 21.4 kcal mol^{-1}. This calculation is further supported by the recent development from Anderson and co-workers who first reported the fusion of an anthracenyl moiety with a porphyrin core.[23] Current work is now focused toward the development of new synthetic methodologies to synthesize newly fused multianthracenyl-porphyrin derivatives.

Electrochemiluminescence measurements

ECL measurements were performed according to the method of the co-reactant.[49,50,51] Fig. 11 displays the ECL spectra of compounds **1a–b** and **3** obtained in THF solutions. While the anodic oxidation of **3** in the presence of $i\mathrm{Pr_3N}$ as a co-reactant displays a negligible ECL emission, molecule **1a** produces an ECL spectrum that, in agreement with the fluorescence spectrum, displays a shoulder peak at 603 nm and a maximum at 654 nm. The free energy of the reaction of the porphyrin radical cation with the electrogenerated $i\mathrm{Pr_3N}$ radical (*i.e.*, 0.96 + 1.1 = 2.06 eV) is close to the level needed to populate the singlet state of the porphyrin, thus suggesting that both S- and T-routes are viable for the generation of ECL. Surprisingly, in spite of the very similar oxidation potentials of porphyrins **1a–b**, ECL was largely suppressed in molecule **1b**. This contrasts with the behaviour of other systems recently reported, such as phenyl-2-quinolinylethynes,[52] where the presence of strong donor groups on the phenyl moiety was found to be essential for promoting ECL. The partial localisation of the oxidation process in **1b** on the lateral anthracenyl units provides a possible rationale for the observed behaviour. The oxidised anthracenyl unit provides a viable route to the quenching of the porphyrin-centred excited state. On the other hand, the formation of anthracene-centred excited state, which may be expected from the reaction of **1b** radical cation with the electrogenerated $i\mathrm{Pr_3N}$ radical, is energetically unfavoured (energy-deficient reaction) and so it does not occur.

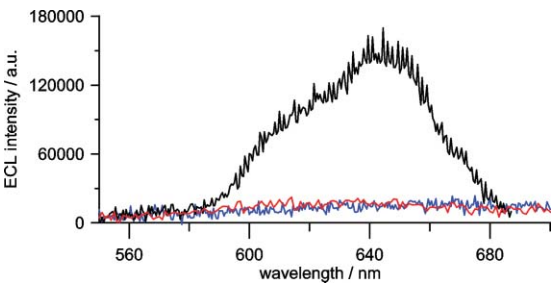

Fig. 11 ECL spectra of 0.5 mM **3** (red line), **1a** (black line), and **1b** (blue line) in THF solutions (+5 mM $i\mathrm{Pr_3N}$) obtained by pulsing the Pt electrode between 0.0 and 1.8 V *vs.* Ag/AgCl at 1 Hz.

Conclusions

A protocol for synthesizing newly designed anthracenyl-porphyrin derivatives (**1a–b**) *via* a Suzuki-type cross-coupling reaction has been developed. Moreover, functional groups, such as *N*,*N*-dimethylaniline, are readily attached to the lateral position of the anthracenyl derivative, offering new ways to tune the physicochemical properties. Steady-state absorption spectra of the porphyrin conjugates reveal some degree of delocalisation with the directly linked chromophores, particularly in the case of anthracenyl-porphyrin bearing dimethylanilino moieties at the two extremities (**1b**). Fluorescence and 77 K phosphorescence measurements show that the excitation energy is invariably funnelled to the lowest singlet and triplet states of the porphyrin chromophore. The latter levels have been monitored also by transient absorption spectroscopy, showing the typical triplet features detected in *meso*-substituted porphyrins. Multiple reversible redox processes were observed by means of CV measurements for both anthracenyl-porphyrin molecules. The presence of the two peripheral *N*,*N*-dimethylanilino residues in molecule **1b** lead to dramatic changes in the anodic region of the CV curve. In particular, for molecule **1a** the two first oxidations occur at the tetrapyrrolic ring being the HOMO and HOMO-1 located at the porphyrin core, whereas for porphyrin **1b** the first two oxidations (*i.e.*, at 0.94 and 1.04 V) take place at the tetrapyrrolic and anthracenyl moieties respectively. By means of UV-Vis-NIR spectroelectrochemical measurements, a NIR-centred intramolecular photoinduced intervalence charge transfer (IV-CT) from a neutral *N*,*N*-dimethylanilino moiety to the *N*,*N*-dimethylanilino radical cation has also been observed for the doubly-oxidised porphyrin derivative $\mathbf{1b}^{2+}$. The latter charge transfer is most probably occurring through a planarised quinoidal-like structure. By means of the method of the co-reactant using electrogenerated $i\mathrm{Pr_3N}$ radical it has been shown that compound **1a** displays good ECL properties. Surprisingly, in spite of the very similar oxidation potentials of porphyrins **1a–b**, ECL was virtually suppressed in molecule **1b**. The new anthracenyl-porphyrin derivatives reported here are promising molecular modules for further scaffolding in either one or two-dimensions. Indeed, future work will focus on the development of new synthetic methodologies to further expand the π-conjugation of the central tetrapyrrolic ring *via* oxidative fusion of the anthracenyl moieties to prepare extended, bi-dimensional, porphyrin-based materials.

Experimental section

Photophysics

Absorption spectra were recorded with a Perkin-Elmer λ40 spectrophotometer. Emission spectra were obtained with an Edinburgh FLS920 spectrometer (continuous 450 W Xe lamp), equipped with a Peltier-cooled Hamamatsu R928 photomultiplier tube (185–850 nm). Emission quantum yields were determined according to the approach described by Demas and Crosby[53] using [Ru(bipyridine)$_3$Cl$_2$] (Φ_{em} = 0.028 in air-equilibrated H_2O solution)[54] as standard. Emission lifetimes of the species absorbing in the UV and VIS regions were determined with two spectrometers using the time correlated single photon counting technique with different sources (thyratron gated N_2 lamp at

308 or 337 nm and laser diode at 407 nm), setup details are reported elsewhere.[55] Phosphorescence spectra and related long-lived decay signals (s-ms timescale) were recorded with a Perkin-Elmer LS-50B spectrofluorimeter, equipped with a Hamamatsu R928 PMT. Transient absorption spectra and lifetimes were detected upon excitation at 532 nm (Nd:YAG laser); details on the apparatus have been already reported.[55]

Electrochemistry

All chemicals used were reagent grade. Tetrabutylammonium hexafluorophosphate (TBAH, Fluka) was used as supporting electrolyte as received. Tetrahydrofuran (LiChrosolv) was treated according to a procedure described elsewhere.[56] For the voltammetric experiments, the solvent was distilled into the electrochemical cell, prior to use, by a trap-to-trap procedure. In the voltammetric experiments, a one-compartment electrochemical cell of airtight design was used, with high-vacuum glass stopcocks fitted with Viton (DuPont) O-rings to prevent contamination by grease. The connections to the high-vacuum line and to the Schlenk flask containing the solvent were made by spherical joints fitted with Viton O-rings. The pressure measured in the electrochemical cell prior to performing the trap-to-trap distillation of the solvent was typically $1.0–2.0 \cdot 10^{-5}$ mbar. The working electrode consisted of platinum disk ultramicroelectrodes (with radius = 62.5 μm) also sealed in glass. The counter electrode consisted of a platinum spiral, and the quasi-reference electrode was a silver spiral. The quasi-reference electrode drift was negligible for the time required by a single experiment. Both the counter and reference electrodes were separated from the working electrode by ~0.5 cm. Potentials were measured with the ferrocene or decamethylferrocene standards and are always referred to saturated calomel electrode (SCE). $E_{1/2}$ values correspond to $(E_{pc} + E_{pa})/2$ from CV. Ferrocene was also used as an internal standard for checking the electrochemical reversibility of a redox couple. The temperature dependence of the relevant internal standard redox couple potential was measured with respect to SCE by a nonisothermal arrangement.[57] Voltammograms were recorded with an AMEL Model 552 potentiostat or a custom-made fast potentiostat controlled by either an AMEL Model 568 function generator or an ELCHEMA Model FG-206F. Data acquisition was performed by a Nicolet Model 3091 digital oscilloscope interfaced to a PC. Temperature control was accomplished within 0.1 °C with a Lauda thermostat. The minimization of ohmic drop was achieved through the positive feedback circuit implemented in the potentiostat. ECL was generated by a single oxidative step according to well established methods.[51] The ECL signal during cyclic voltammetry was measured with a photomultiplier tube (PMT, Hamamatsu R4220p) placed a few millimetres in front of the working electrode inside a darkbox with the detector entrance hole including completely the surface of working electrode. A voltage of 1000 V was supplied to the PMT. To register light/current/voltages curves PMT output signal was sent to a current ultra low noise preamplifier (Acton research mod. 181). After electronic processing the signal is directly sent to the second input channel of AUTOLAB. For these types of measurements PMT was biased at 750 V. ECL spectra were recorded by inserting the same PMT in a dual exit monochromator (ACTON RESEARCH mod. spectra pro 2300i). Photocurrent detected at PMT was accumulated for 3 to 5 seconds depending on emission intensity, for each monochromator step; entrance and exit slits were fixed to the maximum value of 3 mm.

Computational studies

The computational models of **1a** and **1b** and their derivatives were constructed by replacing the 3,5-di(*tert*-butyl)phenyl groups replaced by H atoms. Geometry optimizations of all the complexes were performed at the DFT/BLYP[31,32] level of theory using the program CPMD,[30] with a plane waves (PW) basis set up to an energy cutoff of 70 Ry. Core/valence interactions were described using norm conserving pseudopotentials of the Martins–Troullier type.[58] Periodic boundary conditions were applied and we have used orthorhombic cells of the edge of $a = 35.0$ Å, $b = 15.0$ Å, and $c = 15.0$ Å for **1a** (and its oxidised derivatives) and of $a = 24.0$ Å, $b = 12.0$ Å, and $c = 12.0$ Å for **1b**, its oxidised derivatives as well as the products deriving from the oxidative fusion **8**. Isolated system conditions[59] were applied. Geometries of complexes **1a** and **1b** were also optimised with Gaussian[33] without symmetry constraints at the B3LYP/6-31G(d) level.[32,34]

Synthesis

NMR spectra were obtained on a Varian Gemini 200 spectrometer (200 MHz ^{1}H-NMR and 50 MHz ^{13}C-NMR) and on a Jeol JNM-EX400 (400 MHz ^{1}H-NMR). Chemical shifts are reported in ppm using the solvent residual signal as an internal reference ($CDCl_3$: $\delta_H = 7.26$ ppm, $\delta_C = 77.16$ ppm; CD_3OD: $\delta_H = 3.31$ ppm, $\delta_C = 49.00$ ppm; C_5D_5N: $\delta_H = 7.19, 7.55, 8.71$ ppm, $\delta_C = 123.5, 135.5, 149.5$ ppm; $(CD_3)_2SO$: $\delta_H = 2.50$ ppm, $\delta_C = 39.52$ ppm). Coupling constants (J) are given in Hz. The resonance multiplicity is described as *s* (singlet), *d* (doublet), *t* (triplet), *q* (quartet), *dd* (doublet of doublets), *m* (multiplet), *br* (broad signal). IR spectra (KBr) were recorded on a Perkin Elmer 2000 spectometer by Mr Paolo de Baseggio. Mass spectrometry measurements: Electrospray Ionization (ESI) performed on a Perkin-Elmer API1 at 5600 eV and Electron Impact (EI) performed on a Ion trap GCQ Finnigan Thermoquest at 70 eV were recorded at Università degli Studi di Trieste by Dr Fabio Hollan. Melting Points (m.p.) were measured on a Büchi SMP-20. Chemicals were purchased from, Aldrich, Fluka and Riedel and used as received. Solvents were purchased from JTBaker and Aldrich, and deuterated solvents from Cambridge Isotope Laboratories. The solutions were degassed following the "freeze–pump–thaw" cycles methodology. General solvents such as CH_2Cl_2, PhMe, THF, and NEt_3 were distilled from Na, Na/benzophenone, and CaH_2 respectively. For the synthesis of the single compounds see the ESI.†

Acknowledgements

This work was supported by the European Union through the Marie-Curie Research Training Network "PRAIRIES", contract MRTN-CT-2006–035810, Marie-Curie Initial Training Network "FINELUMEN", grant agreement PITN-GA-2008–215399, the University of Trieste, the University of Bologna, the University of Namur, INSTM, MIUR (PRIN 2006, prot. 20064372 and 2006034018, FIRB, prot. RBIN04HC3S), the Belgian National Research Foundation (FRS-FNRS, through

the contracts n° 2.4.625.08.F and 2.4.550.09.F), and the CNR (commessa PM.P04.010, MACOL). We thank Dr Fabio Hollan (University of Trieste) for the mass spectrometry measurements. SG thanks Dr Mara Campagnolo for help in the acquisition of the X-ray data.

References

1 F. Diederich, *Chem. Commun.*, 2001, 219.
2 R. E. Martin and F. Diederich, *Angew. Chem. Int. Ed.*, 1999, **38**, 1350; J. S. Wu, W. Pisula and K. Müllen, *Chem. Rev.*, 2007, **107**, 718; Y. Nakamura, N. Aratani and A. Osuka, *Chem. Soc. Rev.*, 2007, **36**, 831; K. Müllen and J. P. Rabe, *Acc. Chem. Res.*, 2008, **41**, 511.
3 L. J. Zhi and K. Müllen, *J. Mater. Chem.*, 2008, **18**, 1472; A. C. Grimsdale and K. Müllen, *Angew. Chem. Int. Ed.*, 2005, **44**, 5592; D. Kim and A. Osuka, *Acc. Chem. Res.*, 2004, **37**, 735.
4 M. A. Baldo, D. F. O'Brien, Y. You, A. Shoustikov, S. Sibley, M. E. Thompson and S. R. Forrest, *Nature*, 1998, **395**, 151.
5 U. Mitschke and P. Bauerle, *J. Mater. Chem.*, 2000, **10**, 1471.
6 C. Borek, K. Hanson, P. Djurovich, M. Thompson, K. Aznavour, R. Bau, Y. Sun, S. Forrest, J. Brooks, L. Michalski and J. Brown, *Angew. Chem. Int. Ed.*, 2007, **46**, 1109; B. S. Li, J. Li, Y. Q. Fu and Z. S. Bo, *J. Am. Chem. Soc.*, 2004, **126**, 3430; N. E. Tokel, C. P. Keszthelyi and A. J. Bard, *J. Am. Chem. Soc.*, 1972, **94**, 4872.
7 V. Cleave, G. Yahioglu, P. Le Barny, D. H. Hwang, A. B. Holmes, R. H. Friend and N. Tessler, *Adv. Mater.*, 2001, **13**, 44.
8 A. K. Burrell, D. L. Officer, P. G. Plieger and D. C. W. Reid, *Chem. Rev.*, 2001, **101**, 2751.
9 H. L. Anderson, *Chem. Commun.*, 1999, 2323.
10 Z. M. Liu, A. A. Yasseri, J. S. Lindsey and D. F. Bocian, *Science*, 2003, **302**, 1543; K. S. Chichak, A. Star, M. V. R. Altoe and J. F. Stoddart, *Small*, 2005, **1**, 452.
11 D. F. O'Brien, C. Giebeler, R. B. Fletcher, A. J. Cadby, L. C. Palilis, D. G. Lidzey, P. A. Lane, D. D. C. Bradley and W. Blau, *Synthetic Met.*, 2001, **116**, 379; E. Pinotti, M. Cartotti, A. Sassella and A. Borghesi, *Synthetic Met.*, 2007, **157**, 1029; H. A. Collins, M. Khurana, E. H. Moriyama, A. Mariampillai, E. Dahlstedt, M. Balaz, M. K. Kuimova, M. Drobizhev, V. X. D. Yang, D. Phillips, A. Rebane, B. C. Wilson and H. L. Anderson, *Nat. Photonics*, 2008, **2**, 420; H. Tanaka, T. Yajima, T. Matsumoto, Y. Otsuka and T. Ogawa, *Adv. Mater.*, 2006, **18**, 1411; H. Ji, J. Hu and L. Wan, *Chem. Commun.*, 2008, 2653; C. Y. Liu and A. J. Bard, *Electrochem. Solid. St.*, 2001, **4**, E39; B. R. Takulapalli, G. M. Laws, P. A. Liddell, J. Andreasson, Z. Erno, D. Gust and T. J. Thornton, *J. Am. Chem. Soc.*, 2008, **130**, 2226; H. Imahori, K. Mitamura, Y. Shibano, T. Umeyama, Y. Matano, K. Yoshida, S. Isoda, Y. Araki and O. Ito, *J. Phys. Chem. B*, 2006, **110**, 11399; D. M. Guldi, I. Zilbermann, G. A. Anderson, K. Kordatos, M. Prato, R. Tafuro and L. Valli, *J. Mater. Chem.*, 2004, **14**, 303; Y. Noguchi, R. Ueda, T. Kubota, T. Kamikado, S. Yokoyama and T. Nagase, *Thin Solid Films*, 2008, **516**, 2762.
12 L. Karki, F. W. Vance, J. T. Hupp, S. M. LeCours and M. J. Therien, *J. Am. Chem. Soc.*, 1998, **120**, 2606; S. M. LeCours, S. G. DiMagno and M. J. Therien, *J. Am. Chem. Soc.*, 1996, **118**, 11854; S. M. LeCours, H. W. Guan, S. G. DiMagno, C. H. Wang and M. J. Therien, *J. Am. Chem. Soc.*, 1996, **118**, 1497; A. Forneli, M. Planells, M. A. Sarmentero, E. Martinez-Ferrero, B. C. O'Regan, P. Ballester and E. Palomares, *J. Mater. Chem.*, 2008, **18**, 1652.
13 J. S. Lindsey and R. W. Wagner, *J. Org. Chem.*, 1989, **54**, 828.
14 N. Aratani and A. Osuka, *Org. Lett.*, 2001, **3**, 4213; P. N. Taylor, J. Huuskonen, G. Rumbles, R. T. Aplin, E. Williams and H. L. Anderson, *Chem. Commun.*, 1998, 909; F. C. Grozema, C. Houarner-Rassin, P. Prins, L. D. A. Siebbeles and H. L. Anderson, *J. Am. Chem. Soc.*, 2007, **129**, 13370.
15 M. Ezoe, T. Minami, Y. Ogawa, S. Yagi, H. Nakazumi, T. Matsuyama, K. Wada and H. Horinaka, *Photoch. Photobio. Sci.*, 2005, **4**, 641; M. Linke-Schaetzel, C. E. Anson, A. K. Powell, G. Buth, E. Palomares, J. D. Durrant, T. S. Balaban and J. M. Lehn, *Chem. Eur. J.*, 2006, **12**, 1931; M. Morisue, N. Haruta, D. Kalita and Y. Kobuke, *Chem. Eur. J.*, 2006, **12**, 8123; D. Bonifazi and F. Diederich, *Chem. Commun.*, 2002, 2178.
16 H. L. Anderson, A. P. Wylie and K. Prout, *J. Chem. Soc. Perkin Trans. 2*, 1998, 1607.
17 T. V. Duncan, S. P. Wu and M. J. Therien, *J. Am. Chem. Soc.*, 2006, **128**, 10423; J. Wytko, V. Berl, M. McLaughlin, R. R. Tykwinski, M. Schreiber, F. Diederich, C. Boudon, J. P. Gisselbrecht and M. Gross, *Helv. Chim. Acta*, 1998, **81**, 1964; A. Tsuda and A. Osuka, *Adv. Mater.*, 2002, **14**, 75; T. Ikeue, N. Aratani and A. Osuka, *Isr. J. Chem.*, 2005, **45**, 293; N. P. Redmore, I. V. Rubtsov and M. J. Therien, *J. Am. Chem. Soc.*, 2003, **125**, 8769; J. Song, S. Y. Jang, S. Yamaguchi, J. Sankar, S. Hiroto, N. Aratani, J. Shin, S. Easwaramoorthi, K. S. Kim, D. Kim, H. Shinokubo and T. Osuka, *Angew. Chem. Int. Ed.*, 2008, **47**, 6004; L. Fendt, H. Fang, M. Plonska-Brzezinska, S. Zhang, F. Cheng, C. Braun, L. Echegoyen and F. Diederich, *Eur. J. Org. Chem.*, 2007, 4659.
18 M. Yoon, Z. S. Yoon, S. Cho, D. Kim, A. Takagi, T. Matsumoto, T. Kawai, T. Hori, X. Peng, N. Aratani and A. Osuka, *J. Phys. Chem. A*, 2007, **111**, 9233; T. Hori, X. Peng, N. Aratani, A. Takagi, T. Matsumoto, T. Kawai, Z. S. Yoon, M. Yoon, J. Yang, D. Kim and A. Osuka, *Chem. Eur. J.*, 2008, **14**, 582; Y. Nakamura, N. Aratani, H. Shinokubo, A. Takagi, T. Kawai, T. Matsumoto, Z. S. Yoon, D. Y. Kim, T. K. Ahn, D. Kim, A. Muranaka, N. Kobayashi and A. Osuka, *J. Am. Chem. Soc.*, 2006, **128**, 4119.
19 F. Diederich and B. Felber, *Proc. Natl. Acad. Sci. Usa*, 2002, **99**, 4778; B. Felber, C. Calle, P. Seiler, A. Schweiger and F. Diederich, *Org. Biomol. Chem.*, 2003, **1**, 1090; M. Hoffmann, J. Karnbratt, M. Chang, L. M. Herz, B. Albinsson and H. L. Anderson, *Angew. Chem. Int. Ed.*, 2008, **47**, 4993; M. Hoffmann, C. J. Wilson, B. Odell and H. L. Anderson, *Angew. Chem. Int. Ed.*, 2007, **46**, 3122.
20 J. P. Fillers, K. G. Ravichandran, I. Abdalmuhdi, A. Tulinsky and C. K. Chang, *J. Am. Chem. Soc.*, 1986, **108**, 417.
21 S. Nakajima and A. Osuka, *Tetrahedron Lett.*, 1995, **36**, 8457; J.-M. Cense and R.-M. Le Quan, *Tetrahedron Lett.*, 1979, 3725.
22 S. G. Dimagno, V. S. Y. Lin and M. J. Therien, *J. Org. Chem.*, 1993, **58**, 5983.
23 N. K. S. Davis, M. Pawlicki and H. L. Anderson, *Org. Lett.*, 2008, **10**, 3945.
24 A. Nakano, H. Shimidzu and A. Osuka, *Tetrahedron Lett.*, 1998, **39**, 9489.
25 D. Bonifazi, G. Accorsi, N. Armaroli, F. Song, A. Palkar, L. Echegoyen, M. Scholl, P. Seiler, B. Jaun and F. Diederich, *Helv. Chim. Acta*, 2005, **88**, 1839.
26 N. Armaroli, G. Marconi, L. Echegoyen, J. P. Bourgeois and F. Diederich, *Chem. Eur. J.*, 2000, **6**, 1629.
27 Y. Leydet, D. M. Bassani, G. Jonusauskas and N. D. McClenaghan, *J. Am. Chem. Soc.*, 2007, **129**, 8688.
28 B. Ventura, L. Flamigni, G. Marconi, F. Lodato and D. L. Officer, *New J. Chem.*, 2008, **32**, 166; L. Flamigni, A. M. Talarico, B. Ventura, R. Rein and N. Solladie, *Chem. Eur. J.*, 2006, **12**, 701.
29 N. Armaroli, G. Accorsi, F. Song, A. Palkar, L. Echegoyen, D. Bonifazi and F. Diederich, *ChemPhysChem*, 2005, **6**, 732.
30 J. Hutter, A. Alavi, T. Deutsch, P. Ballone, M. Bernasconi, P. Focher, and S. Goedecker, in '*CPMD*', Stuttgart, 1995.
31 A. D. Becke, *Phys. Rev. A*, 1998, **38**, 3098.
32 C. Lee, W. Yang and R. G. Parr, *Phys. Rev. B*, 1988, **37**, 785.
33 M. J. Frisch, G. W. Trucks, H. B. Schlegel, G. E. Scuseria, M. A. Robb, J. R. Cheeseman, J. A. Montgomery, T. Vreven, K. N. Kudin, J. C. Burant, J. M. Millam, S. S. Iyengar, J. Tomasi, V. Barone, B. Mennucci, M. Cossi, G. Scalmani, N. Rega, G. A. Petersson, H. Nakatsuji, M. Hada, M. Ehara, K. Toyota, R. Fukuda, J. Hasegawa, M. Ishida, T. Nakajima, Y. Honda, O. Kitao, H. Nakai, M. Klene, X. Li, J. E. Knox, H. P. Hratchian, J. B. Cross, V. Bakken, C. Adamo, J. Jaramillo, R. Gomperts, R. E. Stratmann, O. Yazyev, A. J. Austin, R. Cammi, C. Pomelli, J. W. Ochterski, P. Y. Ayala, K. Morokuma, G. A. Voth, P. Salvador, J. J. Dannenberg, V. G. Zakrzewski, S. Dapprich, A. D. Daniels, M. C. Strain, O. Farkas, D. K. Malick, A. D. Rabuck, K. Raghavachari, J. B. Foresman, J. V. Ortiz, Q. Cui, A. G. Baboul, S. Clifford, J. Cioslowski, B. B. Stefanov, G. Liu, A. Liashenko, P. Piskorz, I. Komaromi, R. L. Martin, D. J. Fox, T. Keith, M. A. Al-Laham, C. Y. Peng, A. Nanayakkara, M. Challacombe, P. M. W. Gill, B. Johnson, W. Chen, M. W. Wong, C. Gonzalez and J. A. Pople, in '*Gaussian 03, Revision C.02*', Wallingford, 2004.
34 A. D. Becke, *J. Phys. Chem.*, 1993, **98**, 5648.
35 A. Magistrato, J. VandeVondele and U. Rothlisberger, *Inorg. Chem.*, 2000, **39**, 5553.
36 In 'Kohns Sham orbitals especially those referring to unoccupied states are reported only for a qualitative discussion'.
37 A. M. Stolzenberg, S. W. Simerly, B. D. Steffey and G. S. Haymond, *J. Am. Chem. Soc.*, 1997, **119**, 11843; K. M. Kadish, E. Van Caemelbecke, F. D'Souza, C. J. Medforth, S. Fukuzumi and I. Nakanishi, *Inorg. Chem.*, 1999, **38**, 2188.

38 C.-W. Huang, K. Y. Chiu and S.-H. Cheng, *J. Chem. Soc. Dalton Trans.*, 2005, 2417.
39 M. Wolszczak, M. Steblecka and M. Hilczer, *Chem. Phys. Lett.*, 2005, **410**, 213–217.
40 S. Marquis, A. Moissette and C. C. Brémard, *ChemPhysChem*, 2006, **7**, 1525.
41 M. T. Barton, N. M. Rowley, P. R. Ashton, C. J. Jones, N. Spencer, M. S. Tolley and J. L. Yellowlees, *New J. Chem.*, 2000, **24**, 555.
42 K. M. Kadish, M. M. Franzen, B. C. Han and C. Araullo-McAdams, *J. Am. Chem. Soc.*, 1991, **113**, 512; A. B. J. Parusel, T. Wondimagegn and A. Ghosh, *J. Am. Chem. Soc.*, 2000, **12**, 6371; R. E. Haddad, S. Gazeau, J. Pècaut, J.-C. Marchon, C. J. Medforth and J. A. Shelnutt, *J. Am. Chem. Soc.*, 2003, **125**, 1253.
43 M. T. Barton, N. M. Rowley, P. R. Ashton, C. J. Jones, N. Spencer, M. S. Tolley and J. L. Yellowlees, *J. Chem. Soc. Dalton Trans.*, 2000, 3170–3175.
44 K. Tokumura, N. Mizukami, M. Udagawa and M. Itoh, *J. Phys. Chem.*, 1986, **90**, 3813.
45 D. Chang, T. Malinski, A. Ulman and K. M. Kadish, *Inorg. Chem.*, 1984, **23**, 817; K. M. Kadish, D. Sazou, G. B. Maiya, B. C. Han, Y. M. Liu, A. Saoiabi, M. Ferhat and R. Guilard, *Inorg. Chem.*, 1989, **28**, 2542.
46 L. Flamigni, F. Barigelletti, N. Armaroli, J.-P. Collin, J.-P. Sauvage and J. A. G. Williams, *Chem. Eur. J.*, 1998, **4**, 1744.
47 C. Lambert and G. Nöll, *J. Chem. Soc. Perkin Trans. 2*, 2002, 2039; C. Lambert and G. Nöll, *J. Am. Chem. Soc.*, 1999, **37**, 8434.
48 I. M. Blake, A. Krivokapic, M. Katterle and H. L. Anderson, *Chem. Commun.*, 2002, 1662; I. M. Blake, L. H. Rees, T. D. W. Claridge and H. L. Anderson, *Angew. Chem. Int. Ed.*, 2000, **39**, 1818.
49 L. R. Faulkner, and A. J. Bard, *Electrochemical Methods*, ed. A. J. Bard, New York, 1977; A. W. Knight and G. M. Greenway, *Analyst*, 1994, **119**, 879; A. J. Bard, J. D. Debad, J. K. Leland, G. B. Sigal, J. L. Wilbur, and J. N. Wohlstadter, *Chemiluminescence*, in *Encyclopedia of Analytical Chemistry: Applications, Theory and Instrumentation*, ed. R. A. Meyers, New York, 2000.
50 M. M. Richter, *Chem. Rev.*, 2004, **104**, 3003.
51 A. J. Bard, in '*Electrogenerated chemiluminescence*', ed. M. Dekker, New York, 2004.
52 A. Elangovan, T.-Y. Chen, C.-Y. Chen and T.-I. Ho, *Chem. Commun.*, 2003, 2146.
53 J. N. Demas and G. A. Crosby, *J. Phys. Chem.*, 1971, **75**, 991.
54 S. R. Meech and D. Phillips, *J. Photochem.*, 1983, **23**, 193; S. R. Meech and D. Phillips, *J. Photochem.*, 1983, **23**, 193.
55 K. Hosomizu, H. Imahori, U. Hahn, J. Nierengarten, A. Listorti, N. Armaroli, T. Nemoto and S. Isoda, *J. Phys. Chem. C*, 2007, **111**, 2777.
56 M. Carano, P. Ceroni, L. Mottier, F. Paolucci and S. Roffia, *J. Electrochem. Soc.*, 1999, **146**, 3357.
57 E. L. Yee, R. J. Cave, K. L. Guyer, P. D. Tyma and M. J. Weaver, *J. Am. Chem. Soc.*, 1979, **101**, 1131.
58 N. Trouille and J. L. Martins, *Phys. Rev. B*, 1991, **43**, 1993.
59 R. N. Barnett and U. Landman, *Phys. Rev. B*, 1993, **48**, 2081.